Fault Tolerance Enhancements for Quantum Data Encodings

Aviraj Sinha and Mitchell A. Thornton
Darwin Deason Institute of Cybersecurity
Southern Methodist University, Dallas, TX 75205, USA
Email: {avirajs, mitch}@smu.edu

***Abstract*—Data quality is an important factor in quantum computation, since quantum algorithms need high quality representations in order to run with low error rates. In addition, quantum algorithms benefit from different types of quantum data encodings that are tailored to specific applications. In order to improve data quality while maintaining data variety, this work applies fault tolerance techniques specific to different types of data encodings. Thus, fault tolerance improvements, aimed at reducing both noise and bias errors, are applied to two types of data encodings. The first type, angle encoding, benefits from an enhanced dynamic range representation. The second type, distribution encoding, is enhanced through the use of error correcting states. Our experiments encode classical data as a quantum state, apply noise simulations, and provide error analyses on the decoded data. Experimental results are assessed by comparing the post-processed output statistics to those of the original encodings and show improved accuracy through the inclusion of fault tolerance methods.**

***Index Terms*—Fault tolerance, quantum computing, qubits, data encoding**

I. Introduction

Encoding, error application, and decoding are all steps included in data processing. Encoding involves converting data into a specific format for efficient transmission, storage, or transformation. The channel, either physical or logical, serves as the medium for data transmission, where errors caused by noise, interference, or channel imperfections can alter the data. Shannon's foundational work [1] introduces the concept of information transmission using binary bits, while Peterson's work [2] establishes error correction techniques and encoding methods. Data errors in transmission may manifest as random noise or systematic distortions and can affect metrics such as transmission rate and error rate. Decoding, the process of reconstructing original data, incorporates error correction techniques such as redundancy or parity bits to detect and correct errors. To account for noise, encoding schemes are designed with fault tolerance techniques that detect and correct errors during decoding. These techniques rely on statistical models to estimate the likelihood of errors and apply appropriate corrections. For example, classical error correction codes, such as Hamming codes, use redundancy to identify and rectify errors introduced during transmission [3]. These techniques aim to mitigate the effects of noise, ensuring reliable performance in real-world conditions where disturbances are unavoidable.

This paper introduces an improvement in accurately representing quantum data by leveraging fault tolerance methods specifically designed for specific forms of quantum data encoding that enhance the reliability of quantum algorithms with respect to the presence of noise. Although many previous works exist in quantum fault tolerance, they are focused upon the error correction of quantum binary basis states and the application of quantum error correction circuits [4], [5]. There are several alternative ways of encoding data using other forms of representation that can be improved with fault tolerance approaches. Quantum data encoding quality is crucial for secure and reliable communication in applications such as quantum key distribution (QKD) and quantum teleportation. Multiple simple data encoding methods for quantum channels are described in [6], offering foundational insights into quantum data encoding approaches and how they affect the results of quantum algorithms. By analyzing the robustness of different and more robust data encoding methods, we extend the work of [7] that examines the noise-resilience of basis, angle, and amplitude classes of quantum data encoding. This work focuses on improving two categories of data encoding approaches; those of angle-based encoding that represent data through the phase angle of a qubit, and, distribution-based encoding that represents data using probability amplitudes of a qubit. Each data encoding type has unique challenges posed by quantum noise and requires unique solutions to improve the representation quality.

We enhance the fault tolerance of angle-based data encoding by applying an improved dynamic range representation. Dynamic range encoding addresses dynamic range issues that arise when datasets contain both large and small values, making standard angle encoding methods prone to saturation and underflow. Previous work described the impact of representing multiple data as angles and the effect of normalization [8]. This technique represents data as a mantissa and exponent, similar to classical floating-point values, and encodes them as amplitude and phase angles of a qubit, respectively. By redistributing noise across these components and using a local scaling factor instead of a global one, dynamic range encoding minimizes the impact of individual noise sources, reduces bias errors, and ensures precise data representation. The adaptive boundaries used to decode the integer exponent is also introduced and is optimized using statistical models described in [9], further enhancing fault tolerance by effectively mitigating bias and variance introduced by quantum noise.

Distribution-based data encoding does not represent information as qubit phase angles but instead leverages the inherent randomness of the quantum state to generate probability mass functions (PMFs) [10], [11]. The proposed technique enhances data representation accuracy using fault tolerance methods that exploit Hamming error correction to reduce bitflip errors in the encoded distributions. By introducing zero-probability states between PMF bins as buffers, the Hamming distance increases among representable quantum data values and thus helps to mitigate errors. During the measurement process, nearby quantum states are combined, allowing for the correction of noise-induced bitflips.

To evaluate the effectiveness of these advancements, this work conducts simulations of noisy environments, analyzing the encoded and decoded outputs under varying levels of noise. The evaluation employs statistical metrics such as decoding accuracy and the Kullback-Leibler (KL)-divergence metric, to demonstrate improvements in noise resiliency [9], [12]. The results highlight the capability of dynamic range encoding and the enhanced quantum distribution encoding to handle variations in data values while maintaining precision.

II. Background

Quantum computing relies on the concept of qubits, which are the fundamental data units of quantum computation. Unlike classical bits, which take values of 0 or 1, a qubit can exist in a superposition of two basis states, represented as $|\psi\rangle = \alpha|0\rangle + \beta|1\rangle$, where α and β are complex probability amplitudes satisfying $|\alpha|^2 + |\beta|^2 = 1$. A qubit can also be parameterized using angles to reflect its state on the Bloch sphere as $|\psi\rangle = \cos\left(\frac{\theta}{2}\right)|0\rangle + e^{i\varphi}\sin\left(\frac{\theta}{2}\right)|1\rangle$, where θ and φ are angular parameters representing the position of a quantum state on the Block sphere [13]. Alternatively, the angle φ is defined to be the phase of a qubit. This dual representation emphasizes that data can be represented or encoded as either angles or probabilities.

Each data encoding will require a different decoding process. For example, measurements on a qubit yield counts n_0 and n_1 for observing the states $|0\rangle$ and $|1\rangle$, respectively. From these counts, the angle $\hat{\theta}$ can be reconstructed using the calculation: $\hat{\theta} = 2\arcsin\left(\sqrt{\frac{n_1}{n_0+n_1}}\right)$ and $\hat{\varphi}$ can be extracted through the use of a phase interferometer circuit that precedes the projective measurement operator. Alternatively, the decoding process of a quantum distribution can simply involve the count of multiple measurements of the quantum state and normalized by the total number of counts. Each estimated PMF bin value can be obtained using the calculation $\hat{P}(i) = \frac{n_i}{\sum_j n_j}$, where n_i represents the measured counts for each state, and the summation $\sum_j n_j$ ensures proper normalization across all measured states. These formulations allow for the decoding of different data representations either in terms of angular parameters or probabilities. The choice of decoding method—whether via the arcsin-based angle calculation or probability normalization—depends on the application and the nature of the encoded quantum information.

Different quality metrics are employed for evaluating various data encoding schemes. The robustness of angle encoding is assessed through statistical analysis of the encoded and decoded data under noisy conditions. Key metrics include bias, defined as $\text{Bias} = \mathbb{E}[\hat{\theta}] - \theta$, where $\hat{\theta}$ is the estimated value and θ is the true value, and variance, defined as $\text{Variance} = \mathbb{E}[(\hat{\theta} - \mathbb{E}[\hat{\theta}])^2]$, which quantifies the spread or variability of the decoded data due to random noise. For both metrics, the ideal value is 0, indicating no systematic error (bias) and no variability due to noise (variance). For distribution-based encodings, metrics specifically designed for probability distributions are used. Statistical tests provide quantitative insights into the robustness of these schemes by evaluating the significance of observed differences. One such metric is the KL divergence, defined as $KL(P\|Q) = \sum_i P(i)\ln\frac{P(i)}{Q(i)}$, where $P(i)$ represents the observed probabilities and $Q(i)$ the reference (ideal) probabilities. The KL divergence measures the difference between the observed distribution and a reference distribution, with an ideal value of 0, indicating that the observed and reference distributions are identical. Both bias and variance, as well as KL divergence, are computed by comparing the expected outputs to the decoded outputs obtained after applying noise simulations and conducting multiple measurements. These metrics collectively provide a comprehensive evaluation of the encoding schemes' performance under noisy conditions.

A robust encoding and decoding process ensures that the transmitted information can be accurately reconstructed, even in the presence of significant noise. Encoding schemes often incorporate redundancy or structural features to detect and correct errors during decoding. The goal is to maintain the representation of the original data, minimizing the impact of noise and ensuring reliable performance in practical applications. Following the framework of [7], Equation 1 formalizes the process of encoding and decoding data in a manner resilient to quantum errors. This equation represents how a robust encoding ensures that the information transferred through measurements remains unaffected by the application of errors. The process involves first encoding data into a quantum state, denoted by $\tilde{\rho}_{\boldsymbol{x}}$. Next, an error channel $\mathcal{E}$ is applied, which can be modeled as a set of Kraus operators acting on the quantum state. After the error channel, a decoding procedure $\hat{y}$ is performed, which may include preprocessing and measurement. The robust nature of the encoding is reflected in the equality shown in Equation 1. This equation signifies that applying the error channel $\mathcal{E}$ does not impact the information extracted during measurement when using a robust encoding scheme. In essence, the robustness of the channel ensures that noise introduced by the error process does not degrade the encoded information, preserving its integrity throughout the transmission and processing stages.

$$\hat{y}\left[\mathcal{E}\left(\tilde{\rho}_{\boldsymbol{x}}\right)\right] = \hat{y}\left[\tilde{\rho}_{\boldsymbol{x}}\right], \tag{1}$$

To test the robustness of quantum data encodings under various quantum errors, noise simulations are performed using Kraus operators, which act on the density matrix to model quantum noise and errors [13]–[15]. A Kraus operator E_i transforms a density matrix ρ via $\mathcal{E}(\rho) = \sum_i E_i \rho E_i^\dagger$, ensuring trace preservation and valid quantum state evolution. For example, the Pauli error channel is defined as $\mathcal{E}_{\mathbf{p}}^{\mathrm{P}}(\rho) = p_I \rho + p_X X\rho X + p_Y Y\rho Y + p_Z Z\rho Z$, where $p_I + p_X + p_Y + p_Z = 1$ [16], [17]. This channel models errors of bit flips and phase flips. The bit flip channel is described as $\mathcal{E}_p^{\mathrm{BF}}(\rho) = (1-p)\rho + pX\rho X$, and the phase flip channel as $\mathcal{E}_p^{\mathrm{dephase}}(\rho) = (1-p)\rho + pZ\rho Z$. Advanced errors, such as amplitude and phase damping, represent decoherence caused by environmental interactions. Amplitude damping, which models energy dissipation, is defined by Kraus operators:

$$K_0 = \begin{bmatrix} 1 & 0 \\ 0 & \sqrt{1-\gamma(t)} \end{bmatrix}, \quad K_1 = \begin{bmatrix} 0 & \sqrt{\gamma(t)} \\ 0 & 0 \end{bmatrix},$$

where $\gamma(t) = 1 - e^{-\lambda t}$. When applied to a density matrix ρ, the resulting state is $\rho(t) = K_0 \rho K_0^\dagger + K_1 \rho K_1^\dagger$. These formulations allow researchers to model quantum noise and decoherence, providing critical insights into the design of noise-resilient quantum systems. We will use simulation tools, such as those in Qiskit, to further simplify the simulation of error channels [18].

III. Dynamic Range Encoding Enhancement

Challenges arise in accurately representing datasets with a wide range of values, commonly referred to as a high dynamic range. This issue arises in scenarios where datasets include both very small and very large values, making traditional encoding methods prone to underflow errors during normalization. Since conventional angle encoding is able to represent two datawords per qubit, we introduce dynamic range encoding, which can separate the mantissa (M) and exponent (E) of a floating-point number, normalize the two datawords in the range $(0, 2\pi)$, and then represent them as the amplitude θ and phase φ rotations of the qubit. This encoding method distributes noise-induced errors across multiple components, reducing their overall impact. For example, consider a point $X = 0.0001$ subjected to a bias $\Delta = 0.00005$. Without any noise mitigation, the direct representation results in a 50% bias. The same error rate applied to the mantissa $M = 0.1$ introduces only a minor 0.05% relative change.

To generalize the bias reduction effect, we introduce a calculation shown in Equation 2, which expresses the bias B for dynamic range encoding. The larger the exponent value E, the greater the benefits of using dynamic range encoding due to its ability to scale the representation and minimize the absolute impact of noise. In this formulation, $B(X)$ represents the bias introduced to the full representation X, and $B(M)$ represents the bias associated with the mantissa. Dynamic range encoding scales the bias by b^E, making it more effective in reducing the absolute error when E is large (more negative). While the method can generalize to any positive base $b > 1$, in our experiments, we focus on representing classical values in base 10 ($b = 10$).

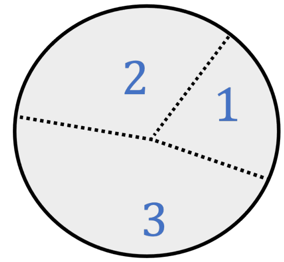

Fig. 1. Adaptive Spacing for Integer Decoding Boundaries

$$\begin{aligned} X &= M \cdot b^E, \quad E \in \mathbb{Z}^-, b > 1, \\ B(M) &= B(X) \cdot b^E. \end{aligned} \tag{2}$$

We will show that the dynamic range encoding confines the integer exponent E, as an angle in a discrete interval. During decoding, the postprocessed angle will be obtained using the method described in Section II. The angle falls within predefined boundaries, enhancing fault tolerance in dynamic range encoding by allowing larger intervals to classify an angle as a specific integer, accommodating greater margins of error. The decoding process is further enhanced through adaptively spaced boundaries, as shown in Figure 1. By interpreting the decoding of angle values as classification through boundaries, noise and bias errors are mitigated effectively. Statistical models, such as Gaussian Mixture Models (GMMs), are employed to analyze noisy measurement data and define robust decoding intervals. The GMM processes uses multiple measurements of quantum states, decodes them into angles, and repeats this to calculate distribution parameters—mean and variance. These parameters define Gaussian curves, with their intersections forming the optimized boundaries. The benefit of adaptive boundaries comes from their ability to address inherent biases that occur on quantum computers due to decoherence, which biases the quantum state to the ground state. Decoherence is modeled through the previously discussed dephasing and damping errors, as referenced in Section II.

The standard integer decoding process associates each interval with an evenly spaced angle. For example, negative exponents $0, -1, -2, -3$ are mapped to boundary angles between $0°$ and $180°$. The four sectors created by these boundaries are as follows: $[(0, 45), (45, 90), (90, 135), (135, 180)]$, with boundaries at $45°, 90°$, and $135°$. For our simulation, we extend the range of exponent values E from 0 to -10. We use Qiskit to introduce a random noise error and a dephasing error with a probability $p = 0.05$.

The classification of 1000 decoded angles, each obtained from applying the arcsin formula for 200 measurements, are performed using these ideal boundaries during the decoding process is evaluated and visualized as a confusion matrix in Figure 2. The confusion matrix orders classes corresponding to the integer-encoded exponents, and the misclassifications between nearby states are clearly visible. This misclassification primarily occurs due to the noise-induced shifts in the boundaries, highlighting the limitations of the standard boundary approach under noisy conditions. Note that misclassification occurs for the the higher angles and lower angles, resulting in an accuracy of 0.46. The smaller angles underflow due to noise and the higher angles get moved close together due to bias created by decoherence.

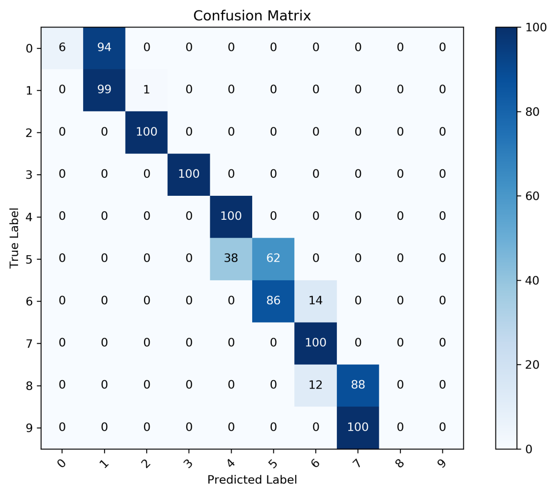

Fig. 2. Confusion matrix for classification under noisy conditions using original boundaries

The previous method, demonstrates the limitations of using static evenly-spaced boundaries in noisy quantum environments. The result highlights the need for adaptive classification techniques to improve the decoding process and mitigate the errors observed in the confusion matrix. For dynamic range encoding with adaptive boundaries, the goal is to train a Gaussian Mixture Model (GMM) to determine optimized boundaries based on statistical information derived from the measurement process. As we did in the standard method, we take 200 measurements of the quantum state, obtain the decoded angle, and calculate a single sample mean x_i. This process is repeated 100 times for each angle representing an integer to evaluate the decoding accuracy. This time we store the multiple samples x_i, and a variance estimate σ_i for each angle i. These parameters define the distributions, with their intersections forming adaptive decoding boundaries that account for noise and bias.

After obtaining the optimized boundaries we can then rerun the simulation to perform classification on the same dataset used to test the original method, using the same decoding and noise simulation settings. Figure 3 visualizes these new adaptive boundaries on the decoding of angles, illustrating how they better accommodate decoherence and other noise effects compared to the static approach especially for the higher quantum states.

Figure 4 presents the confusion matrix for classification using these adaptive boundaries. The results demonstrate a near-perfect classification rate with an accuracy of 0.992, with misclassifications occurring primarily at higher levels, where decoherence has the most significant impact. This improvement indicates the effectiveness of the adaptive boundary method in mitigating noise-induced errors and enhancing the robustness of the decoding process.

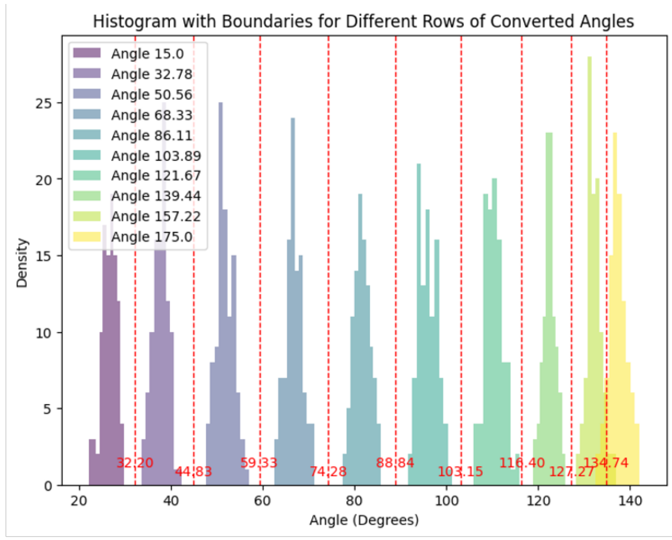

Fig. 3. Improved classification boundaries for noisy angle decoding

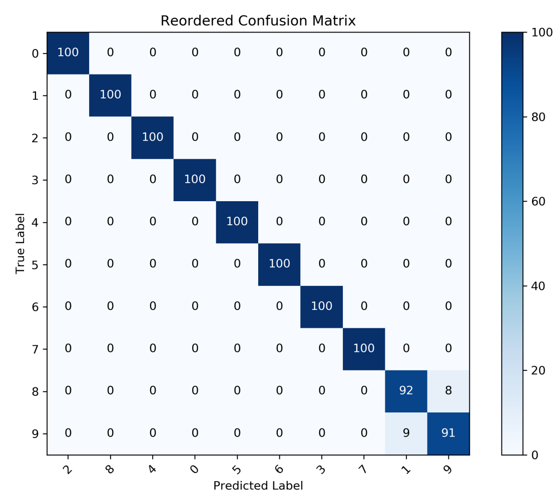

Fig. 4. Confusion matrix for classification using adaptive boundaries under noisy conditions

IV. Enhanced Quantum Distribution Encoding

Using the concepts of Hamming codewords from fault-tolerant computing and probability theory, we propose a method to create robust quantum distribution encodings that are resilient to quantum bitflip errors. Previous methods of generating quantum distributions simply represent each PMF bin as a binary basis state of $|x_n\rangle$ in ascending order with a corresponding probability amplitude $p(x_n)$ [10]. We enhance the previous method by selecting the specific quantum states representing PMF bins to be Hamming codewords that allow for the correction of noisy sampled measurements. We refer to these quantum states representing Hamming codewords as Hamming states. The correction process first checks if the measured quantum state is a valid Hamming codeword, and if the state is not a valid codeword it would be corrected during postprocesing by rounding it to the nearest valid Hamming codeword, in terms of Hamming distance. For testing the improved quality, we can apply the normalization of multiple measurements discussed in Section II.

The process can be described mathematically. We begin by defining the Hamming distance $d(x, y)$, which counts the number of differing positions between two binary vectors x and y. A set $S(x_n)$ is then constructed, which contains all states y that lie within a Hamming distance k from the reference state x_n which is the n-th Hamming state. Next, we can describe how the correction of the measurements results in the improvement of the sample distribution. Let $\hat{P}(n)$ represent the n-th PMF bin of the sample distribution we will obtain after postprocessing and $N(y)$ be the count of a nearby PMF bin and M is the total number of counts in the sample distribution. Over multiple measurements, the correction process combines the nearby states within the set $S(x)$ and normalizes by the total of counts, resulting in the aggregated estimate $\hat{P}(n)$, defined as: $\hat{P}(n) = \frac{1}{M}\sum_{y\in S(x_n)} N(y)$, This operation ensures that measurements of the nearby but slightly differing states are combined, thereby reducing the impact of noisy bitflip errors on the estimated distribution.

We now analyze the effect of bitflip errors on the probability mass function (PMF) representation obtained from multiple measurements of a quantum distribution circuit described in [10]. The random binomial representation is a PMF with 32 bins which are observed by measuring the quantum distribution's 5-qubit output and visualizing the resulting distribution. When bitflip errors are introduced at a rate of $p = 0.05$, we observe a flattening of the PMF curve, as shown in Figure 5. This flattening occurs because bitflip errors cause probability mass to 'leak' into nearby PMF bins, resulting in an increase in uncertainty. The figure highlights this effect by overlaying the noisy PMF distribution on top of the ideal distribution. In addition, the KL divergence is around 0.166, indicating a large quantitative difference between the sample distribution and the ideal distribution.

To mitigate this issue, each quantum state can be associated with a Hamming codeword, which reduces the impact of bitflip errors. To implement this, we use 8 qubits instead of 5, expanding the available state space from $2^5 = 32$ to $2^8 = 256$. However, instead of utilizing all 256 possible states, we restrict the representation to only the 32 valid Hamming codewords, significantly reducing the total percentage of active PMF bins and producing a much sparser representation. This strategy is visualized in Figure 6, which shows the resulting PMF when the same bitflip error rate ($p = 0.05$) is applied to the enhanced quantum distribution's states. Only a subset of 32 possible valid quantum states are used after the correction process, making comparisons to the baseline straightforward. As shown

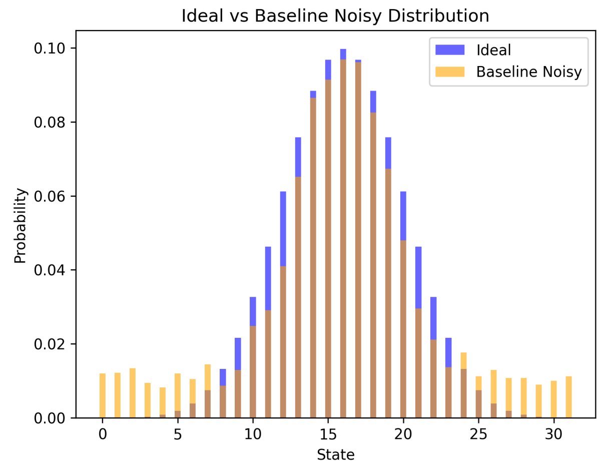

Fig. 5. Quantum distribution PMF with bitflip errors at rate $p = 0.05$. The ideal distribution (blue) is overlaid with the noisy distribution (orange) to highlight the impact of bitflip-induced noise.

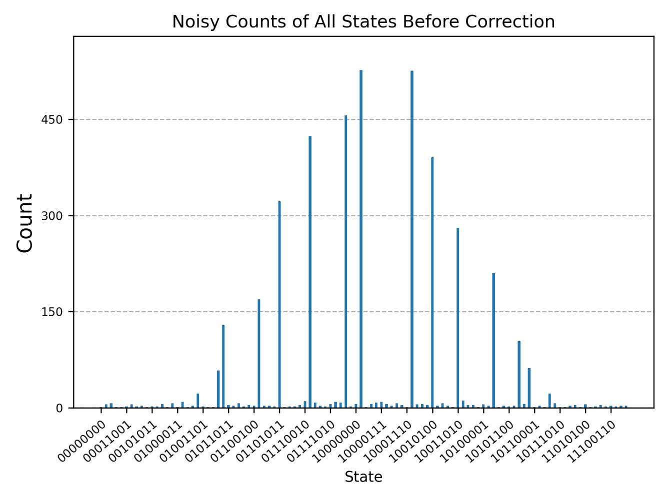

Fig. 6. Quantum distribution PMF with bitflip errors applied to Hamming states of size 8. The sparsity of the PMF is visible, as only valid Hamming codewords are represented, while most non-codeword states have smaller probability.

in the visualization, bitflip errors cause some probability mass to shift into invalid adjacent states. However, these states still lie within a valid Hamming codeword distance that can be corrected. This highlights the error-localizing property of Hamming codes, where errors are confined to neighboring states rather than distant ones, making them easier to detect and correct.

Finally, we introduce the correction process by rounding to the nearest Hamming codewords, effectively "absorbing" the bitflip errors into the closest codeword. Figure 7 illustrates the effect of this process. To achieve this, each noisy state measurement is mapped to the nearest valid Hamming state, and the corresponding probabilities are aggregated into the PMF bin associated with that Hamming codeword. This approach ensures that errors caused by bitflips are corrected as nearby states are combined into a single bin. The visualization demonstrates how the correction process restores the PMF to a shape that closely resembles the ideal distribution. The bins corresponding to valid Hamming codewords are more distinct, and the overall distribution has less variance compared to the noisy distribution seen in Figure 5. When we use the KL-divergence as a metric, we show that it is reduced to 0.0635. This quantitative metric shows that error correction using Hamming state encoding is an effective method for improving fault tolerance in quantum distributions, since the resulting PMF of the same size is closer to the original ideal distribution.

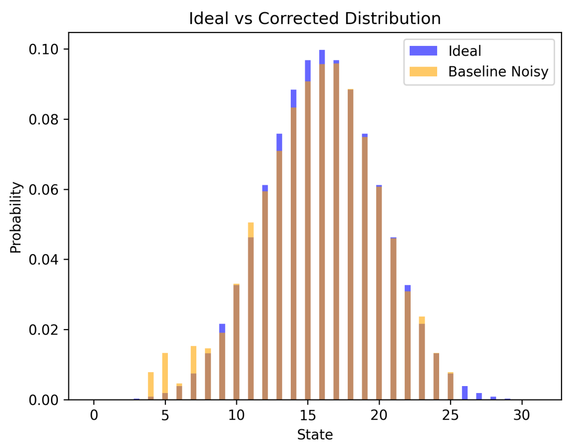

Fig. 7. Hamming state correction after aggregation. The noisy state measurements are aggregated into nearby Hamming codeword bins, resulting in a PMF that closely resembles the ideal distribution.

V. Conclusion

This work presents fault tolerance advancements in angle-based and distribution-based encodings. For angle-based encodings, we introduce a dynamic range representation that separates the mantissa and exponent of floating-point numbers into amplitude and phase rotations. This method redistributes noise across components, reduces bias errors, and ensures precise data representation. Adaptive boundaries optimized using Gaussian Mixture Models (GMMs) further enhance fault tolerance by mitigating the effects of quantum noise. For distribution-based encodings, combining nearby distribution measurements with those of valid Hamming states improve resilience to bitflip errors. Simulations demonstrate significant improvements in fault tolerance highlighting the precision of dynamic range encoding and the enhanced quantum distribution encoding in noisy environments.

In the future, we can improve the compilation and generation of encodings by focusing on optimizing the efficiency of the state generation process, reducing the overall circuit depth, and minimizing gate operations to ensure compatibility with hardware constraints. Additionally, we plan to test the data encoding methods in specific quantum applications, such as quantum machine learning and optimization tasks, to demonstrate improvements in accuracy and computational performance. These efforts will further validate the practical utility of the proposed encodings in real-world scenarios.

References

[1] C. E. Shannon, "A mathematical theory of communication," *Bell System Technical Journal*, vol. 27, no. 3, pp. 379–423, 1948. [Online]. Available: https://ieeexplore.ieee.org/document/6772729

[2] W. W. Peterson and E. J. Weldon, *Error-Correcting Codes*. MIT Press, 1972. [Online]. Available: https://books.google.com/books?id=5kfwlFeklx0C

[3] R. W. Hamming, "Error detecting and error correcting codes," *The Bell system technical journal*, vol. 29, no. 2, pp. 147–160, 1950.

[4] P. W. Shor, "Fault-tolerant quantum computation," in *Proceedings of 37th conference on foundations of computer science*. IEEE, 1996, pp. 56–65.

[5] A. M. Steane, "Error correcting codes in quantum theory," *Physical Review Letters*, vol. 77, no. 5, p. 793, 1996.

[6] M. Schuld, R. Sweke, and J. J. Meyer, "Effect of data encoding on the expressive power of variational quantum-machine-learning models," *Physical Review A*, vol. 103, no. 3, p. 032430, 2021.

[7] R. LaRose and B. Coyle, "Robust data encodings for quantum classifiers," *Physical Review A*, vol. 102, no. 3, p. 032420, 2020.

[8] A. Sinha, E. R. Henderson, J. M. Henderson, and M. A. Thornton, "Automated quantum memory compilation with improved dynamic range," in *2022 IEEE/ACM Third International Workshop on Quantum Computing Software (QCS)*. Los Alamitos, CA, USA: IEEE Computer Society, nov 2022, pp. 22–35. [Online]. Available: https://doi.ieeecomputersociety.org/10.1109/QCS56647.2022.00008

[9] J. R. Hershey and P. A. Olsen, "Approximating the kullback-leibler divergence between gaussian mixture models," in *2007 IEEE International Conference on Acoustics, Speech and Signal Processing (ICASSP)*, 2007, pp. 317–320. [Online]. Available: https://ieeexplore.ieee.org/document/4218101

[10] A. Sinha, E. R. Henderson, J. M. Henderson, E. C. Larson, and M. A. Thornton, "A programmable true random number generator using commercial quantum computers," in *Quantum Information Science, Sensing, and Computation XV*, M. L. Fanto, M. Hayduk, E. Donkor, and C. M. Torres, Eds. SPIE, Jun. 2023. [Online]. Available: https://doi.org/10.1117/12.2663497

[11] M. Schuld, "Supervised quantum machine learning models are kernel methods," *arXiv preprint arXiv:2101.11020*, 2021.

[12] D. A. Reynolds, "Gaussian mixture models," MIT Lincoln Laboratory, Tech. Rep., 2009.

[13] M. A. Nielsen and I. L. Chuang, *Quantum Computation and Quantum Information*. Cambridge University Press, 2000. [Online]. Available: https://books.google.com/books?id=-s4DEy7o-a0C

[14] D. Deutsch, "Quantum theory, the church-turing principle and the universal quantum computer," *Physical Review Letters*, vol. 77, pp. 793–797, 1996. [Online]. Available: https://journals.aps.org/prl/abstract/10.1103/PhysRevLett.77.793

[15] S. J. Devitt, W. J. Munro, and K. Nemoto, "Quantum error correction for beginners," *Reports on Progress in Physics*, vol. 76, p. 076001, 2013. [Online]. Available: https://iopscience.iop.org/article/10.1088/0034-4885/76/7/076001

[16] C. H. Bennett, D. P. DiVincenzo, J. A. Smolin, and W. K. Wootters, "Quantum error correction for arbitrary pauli errors," *Physical Review A*, vol. 55, pp. 1613–1620, 1997. [Online]. Available: https://journals.aps.org/pra/abstract/10.1103/PhysRevA.55.1613

[17] J. Preskill, *Quantum Information and Quantum Computation*. Cambridge University Press, 2004. [Online]. Available: https://books.google.com/books?id=QsBQCBgTx8gC

[18] A. Asfaw, L. Bello, Y. Ben-Haim, S. Bravyi, L. Capelluto, A. C. Vazquez, J. Ceroni, R. Chen, A. Frisch, J. Gambetta, S. Garion, L. Gil, S. D. L. P. González, F. Harkins, T. Imamichi, D. McKay, Z. Minev, P. Nation, A. Phan, M. Pistoia, A. Rattew, J. Schaefer, J. Shabani, J. Smolin, J. A. Smolin, M. Soeken, S. Woerner, and J. Wootton, *Learn Quantum Computing using Qiskit*. Qiskit Community, 2021. [Online]. Available: https://qiskit.org/textbook/